A Bicortical Pedicle Screw in the Cephalad Trajectory Is the Best Option for the Fixation of an Osteoporotic Vertebra: A Finite Element Study

Akimasa Murata[1)], Shunji Tsutsui[1)], Ei Yamamoto[2)], Takuhei Kozaki[1)], Ryuichiro Nakanishi[1)] and Hiroshi Yamada[1)]

1) Department of Orthopaedic Surgery, Wakayama Medical University, Wakayama, Japan
2) Department of Biomedical Engineering, Faculty of Biology-Oriented Science and Technology, Kindai University, Kinokawa, Japan

Abstract:

Introduction: Pedicle screws are commonly used in fixation to treat various spinal disorders. However, screw loosening is a prevalent complication, particularly in patients with osteoporosis. Various biomechanical studies have sought to address this issue, but the optimal depth and trajectory to increase the fixation strength of pedicle screws remain controversial. Therefore, a biomechanical study was conducted using finite element models.

Methods: Three-dimensional finite element models of the L3 vertebrae were developed from the preoperative computed tomography images of nine patients with osteoporosis and nine patients without who underwent spine surgery. Unicortical and bicortical pedicle screws were inserted into the center and into the anterior wall of the vertebrae, respectively, in different trajectories in the sagittal plane: straightforward, cephalad, and caudal. Subsequently, three different external loads were applied to each pedicle screw at the entry point: axial pullout, craniocaudal, and lateromedial loads. Nonlinear analysis was conducted to examine the fixation strength of the pedicle screws.

Results: Irrespective of osteoporosis, the bicortical pedicle screws had greater fixation strength than the unicortical pedicle screws in all trajectories and external loads. The fixation strength of the bicortical pedicle screws was not substantially different among the trajectories against any external loads in the nonosteoporotic vertebrae. However, the fixation strength of the bicortical pedicle screws against craniocaudal load in the cephalad trajectory was considerably greater than those in the caudal (P=0.016) and straightforward (P=0.023) trajectories in the osteoporotic vertebrae. However, this trend was not observed in pullout and lateromedial loads.

Conclusions: Our results indicate that bicortical pedicle screws should be used, regardless of whether the patient has osteoporosis or not. Furthermore, pedicle screws should be inserted in the cephalad trajectory in patients with osteoporosis.

Keywords:

osteoporosis, pedicle screw, depth, trajectory, finite element analysis

Spine Surg Relat Res 2024; 8(5): 510-517
dx.doi.org/10.22603/ssrr.2023-0249

Introduction

Over several decades, pedicle screw (PS) fixation has been a gold standard treatment for various spinal disorders, including degenerative diseases, deformity, and trauma[1-3)]. However, screw loosening is a highly prevalent complication that can result in unfavorable surgical outcomes associated with the loss of spinal alignment or pseudoarthrosis, particularly in patients with osteoporosis[4-8)]. The anchoring ability of PSs depends on the strength of the bone-screw interface; thus, biomechanical studies have been widely conducted to elucidate the factors related to fixation strength (FS), including the morphology of the pedicle, mechanical properties of PSs, and insertion techniques of PSs[9)].

To date, the optimal depth and trajectory of insertion techniques of PSs, particularly in the sagittal plane, remain controversial. From a biomechanical perspective, increasing the length of screws and properly purchasing the anterior vertebral cortex have been advocated as the most secure fixation methods[10)]. Conversely, in the thoracic and lumbar

Corresponding author: Shunji Tsutsui, stsutsui1116@gmail.com
Received: October 3, 2023, Accepted: January 22, 2024, Advance Publication: March 11, 2024

Table 1. Bone Mineral Density and Hounsfield Unit in the O and NO Groups.

Group	BMD (g/cm^3)		HU (L3)
	Femoral neck	Spine	
O	0.568±0.065	0.810±0.128	42.7±23.5
NO	0.773±0.075	0.568±0.065	110.1±37.5

Values are expressed as mean±standard deviation.
BMD, bone mineral density; HU, Hounsfield unit; O, osteoporosis; NO, nonosteoporosis

spines, it has been reported that the pedicle itself contributes to approximately 60% and purchasing of the anterior cortex to 20%-25% of the FS[11]. Regarding the trajectories, screw insertion aimed toward the superior-anterior corner of the vertebral body was shown to provide the best rigidity[12], while screw insertion aimed toward the caudal part of the body in the osteoporotic lumbar vertebrae was reported to provide higher biomechanical strength[13]. These controversies might be attributed to the variations in the properties of specimens used in experiments. Another study that used synthetic osteoporotic bone models with a low material property variance and a homogeneous structural property reported that PSs should be inserted toward the inferior-anterior corner and that there should be purchase of the anterior cortex[14]. However, only the axial pullout force was applied to assess the biomechanical strength of PSs in most previous studies. In a recent biomechanical study that used computational models, axial pullout did not substantially contribute to screw loosening[15]. Furthermore, craniocaudal load was shown to increase the risk of screw loosening in the osteoporotic vertebrae[16]. Therefore, external loading on PSs may be a critical factor for screw loosening. This study used finite element models to explore the optimal depth and trajectory of PSs in the osteoporotic vertebrae against various external loads.

Materials and Methods

The study protocol was reviewed and approved by the ethics committee of our institution. From our database of lumbar spine surgery, 18 female patients aged 55-91 years whose bone mineral densities were measured preoperatively at the femoral neck and spine via dual-energy X-ray absorptiometry were selected. The measurements in the spine with severe degenerative changes were inaccurate; thus, the Hounsfield unit (HU) was used as a substitute, which exhibited correlation with bone mineral density[17-19]. The patients were divided into two groups using the HU: O group (HU≤78.5, n=9), consisting of patients with osteoporosis, and NO group (HU>78.5, n=9), consisting of patients with no osteoporosis[18]. In this study, the L3 vertebra of each patient was used for examinations; thus, the HU values were measured on preoperative computed tomography (CT) images by placing an oval region of interest over three axial slices of L3: immediately inferior to the superior end plate, in the middle of the vertebral body, and superior to the inferior end plate[18]. The HU values from the three slices were averaged. Data about the bone mineral density and HU of each group are summarized in Table 1.

Finite element models

The construction of the finite element models and the biomechanical analyses were conducted using Mechanical Finder (version 11.0, MECHANICAL FINDER, Center for Computational Mechanics, Tokyo, Japan). Three-dimensional finite element models of the L3 vertebrae were constructed using the preoperative CT images of the lumbar spine with a slice thickness of 1 mm. The model consisted of 1-2-mm tetrahedral elements with 39419-86017 nodes and 183872-398737 solid elements[20]. To allow for bone heterogeneity of the vertebra, the mechanical properties of each element were computed from the HU value[20]. To calculate bone density (ρ) from the HU values, the following equation was used:

ρ (g/cm^3)=(HU+1.4246)×0.001/1.058 (If HU>−1)

ρ (g/cm^3)=0.0 (If HU≤−1)

Young's modulus and the yield stress of each tetrahedral element were calculated using the equation utilized by Keyak et al.[21]:

[Young's modulus (E) from bone density (ρ)]

$E=0.001$ ($\rho=0$)

$E=33900\rho^{2.20}$ ($0<\rho\leq0.27$)

$E=5307\rho+469$ ($0.27<\rho<0.6$)

$E=10200\rho^{2.01}$ ($0.6\leq\rho$)

[yield stress (σ_r) from bone density (ρ)]

$\sigma_r=1.0\times10^{20}$ ($\rho\leq0.2$)

$\sigma_r=137\rho^{1.88}$ ($0.2<\rho<0.317$)

$\sigma_r=114\rho^{1.72}$ ($0.317\leq\rho$)

The Poisson's ratio of each element was set to 0.4.

A PS with a 7.0-mm diameter was modeled using the CT data of a PS (MATRIX 5.5 Spine System, DePuy Synthes Spine, Inc., Raynum, MA, USA) taken via a high-resolution micro-CT. The material property of the PS was titanium alloy with Young's modulus of 108.9 GPa, a critical stress of 899 MPa, a yield stress of 824 MPa, and Poisson's ratio of 0.28. The PSs were inserted into the vertebrae through the pedicles. As a result, the models were divided into two solid elements: vertebrae and screws. Based on a previous study, surface-surface contact elements with a frictional coefficient of zero were used for the interface between the PS and the vertebra[22].

Validity of finite element models

As previously reported, a uniformly distributed uniaxial compressive load was applied to the upper surface of the vertebrae, and all elements and nodes on the lower surface were completely constrained[20]. The Newton-Raphson method was employed for nonlinear analysis, and the post-yield modulus was set to 0.05. An element was assumed to yield when its Drucker-Prager equivalent stress reached the element yield stress. Failure in the post-yield phase was de-

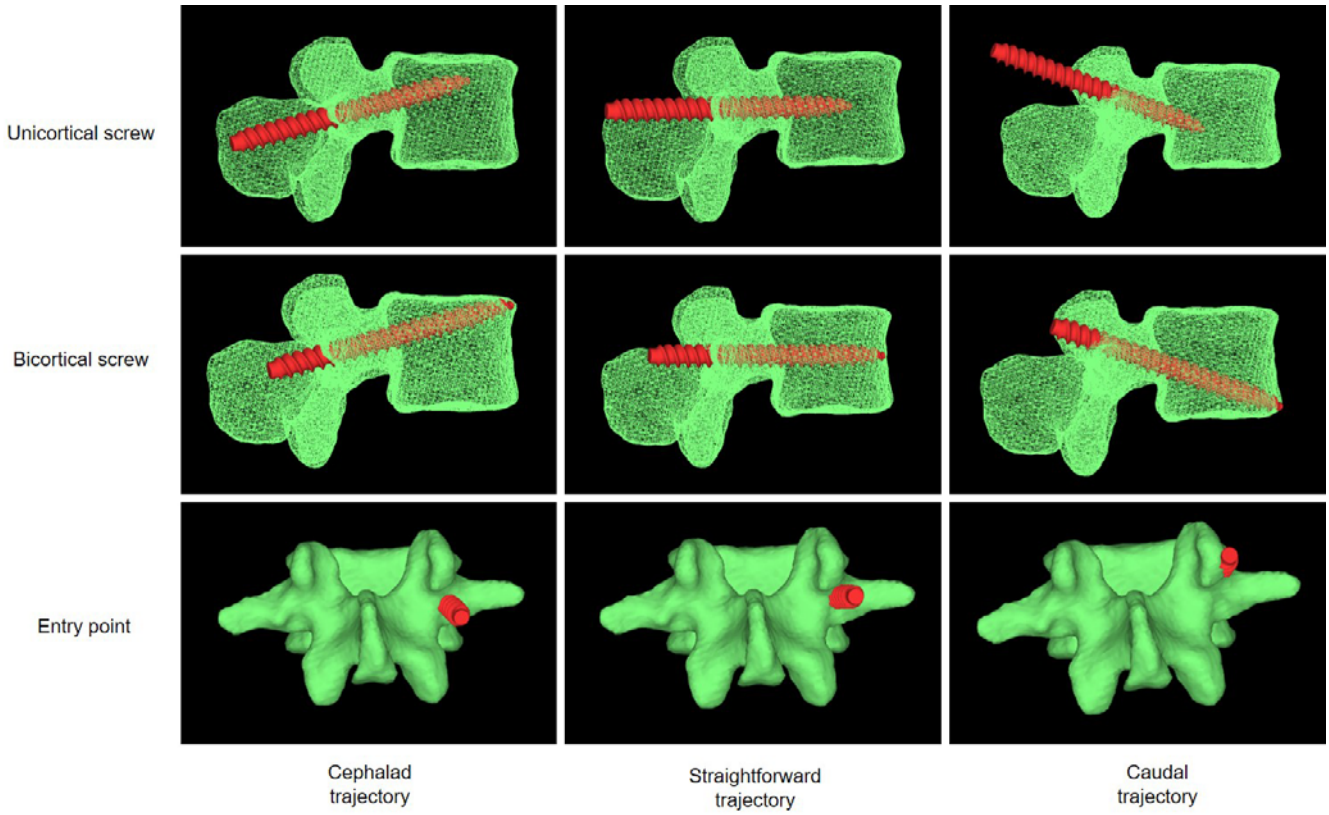

Figure 1. Insertion depth, trajectory, and entry point of the pedicle screws.

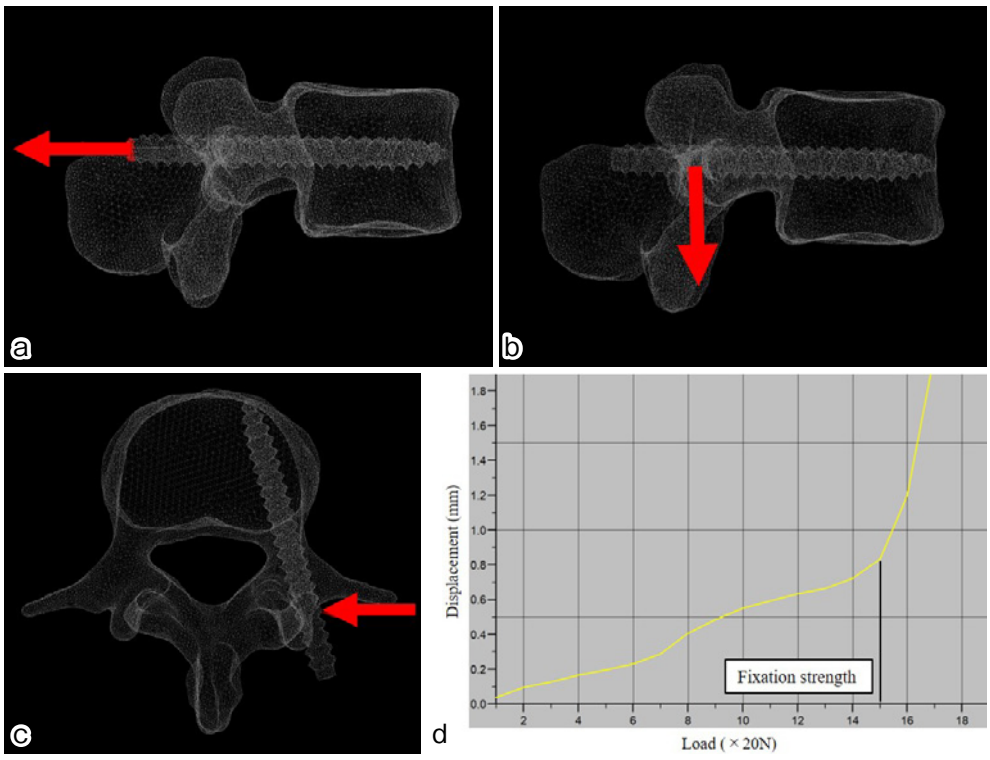

Figure 2. Direction of external loads applied to the pedicle screws (axial pullout [a], craniocaudal [b], and lateromedial [c] loads) and the load–displacement curve displaying the fixation strength of the pedicle screws (d).

fined as a minimum principal strain of the element of less than −10,000 microstrain. Fracture load was defined as the load when at least one element failed. The fracture load in this study was 1,525±904 N, comparable with the value of

Table 2. Fixation Strength (N).

External load	Group	Caudal trajectory			Cephalad trajectory			Straightforward trajectory		
		Unicortical screw	Bicortical screw	*P*	Unicortical screw	Bicortical screw	*P*	Unicortical screw	Bicortical screw	*P*
Axial pullout	O	353.3±128.1	502.2±208.4	0.043*	364.4±129.5	484.4±162.4	0.102	322.2±122.7	406.7±119.2	0.158
	NO	1020.0±530.2	1395.6±781.1	0.250	1066.7±628.6	1408.9±760.7	0.314	948.9±521.5	1200.0±667.5	0.387
Craniocaudal	O	108.9±36.2	200.0±45.8	<0.001*	153.3±40.0	291.1±72.9	<0.001*	120.0±28.3	204.4±70.6	0.004*
	NO	231.1±116.2	417.8±181.5	0.019*	320.0±210.5	526.7±304.0	0.113	235.6±131.1	388.9±207.6	0.079
Lateromedial	O	151.1±60.9	262.2±79.0	0.004*	206.7±86.6	262.2±116.0	0.266	195.6±81.7	2551.1±112.3	0.248
	NO	404.4±209.7	531.1±228.5	0.238	520.0±338.5	688.9±386.5	0.339	473.3±275.9	631.1±309.2	0.270

Values are expressed as mean±standard deviation.
O, osteoporosis; NO, nonosteoporosis
*$P<0.05$ is considered to indicate statistical significance.

1,764±588 N in the previous study[20].

Screw insertion depth and trajectory

The PS insertion techniques employed in this study (Fig. 1) were based on those used in a previous study[14]. PSs with two different lengths were inserted into the vertebrae: unicortical screws to the center and bicortical screws to the anterior cortex of the vertebrae. The PSs were inserted in three different trajectories in the sagittal plane: straightforward (SF) trajectory parallel to the upper endplate of the vertebra, cephalad (CE) trajectory toward the anterior-superior corner of the vertebra, and caudal (CA) trajectory toward the anterior-inferior corner of the vertebra. The entry point for each trajectory was as follows: the intersection of a longitudinal line at the lateral border of the superior articular process with a transverse line bisecting the transverse process for the SF trajectory, a tangential transverse line to the distal border of the transverse process for the CE trajectory, and a tangential transverse line to the proximal border of the transverse process for the CA trajectory. In the axial plane, the PSs were directed 15° toward the midline.

Nonlinear finite element analysis

Nonlinear analysis was conducted to examine the FS of the PSs. Three different external loads were applied to the PSs at the entry point, with the models completely constrained in all directions at the surface of the upper and lower endplates of the vertebrae: axial pullout, craniocaudal, and lateromedial loads (Fig. 2a, b, c). The loading rate was set to 20 N. The load at the sudden inflection point in the load-displacement curve was considered to be FS (Fig. 2d) because at this point, screw displacement rapidly progressed due to bone fracture within the screw threads.

Statistical analyses

Data were expressed as mean±standard deviation. To investigate the optimal depth of PSs and the impact of bone quality on FS, FS was compared using the Mann-Whitney U test between the unicortical and bicortical PSs in each trajectory for both the O and NO groups and between the O and NO groups in each depth or trajectory. Pearson's correlation coefficient was used to explore the correlation between the FS of PSs and the HU values. Furthermore, to investigate the optimal trajectory of PSs, FS was compared via analysis of variance followed by Tukey's post hoc test among the trajectory for each external load. All statistical analyses were conducted using JMP Pro software (version 16; SAS Institute Inc., Cary, NC). $P<0.05$ was considered to indicate statistical significance.

Results

The length (mm) of the unicortical and bicortical PSs were 40.0±0 and 62.1±3.0 mm for the CA, 40.0±0 and 55.0 ±3.1 mm for the SF, and 40.0±0 and 55.6±3.7 mm for the CE trajectories, respectively. Table 2 presents the FS of the PSs in the O and NO groups against each external load for each depth or trajectory. In both groups, the bicortical PSs had greater FS than the unicortical PSs in all trajectories and external loadings. Therefore, the optimal trajectory and impact of osteoporosis on FS of bicortical PSs were investigated. The FS of bicortical PSs was found to be correlated with the HU values in each trajectory (Fig. 3). In the NO group, the FS of the PSs was approximately two- to three-

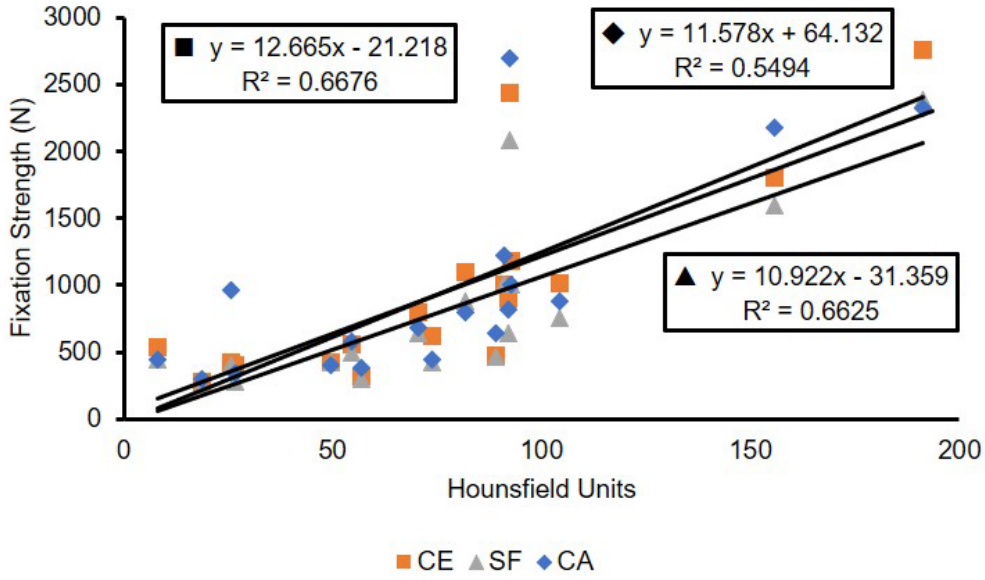

Figure 3. Correlation between the fixation strength of bicortical pedicle screws and Hounsfield unit in the caudal (CA), cephalad (CE), and straightforward (SF) trajectories.

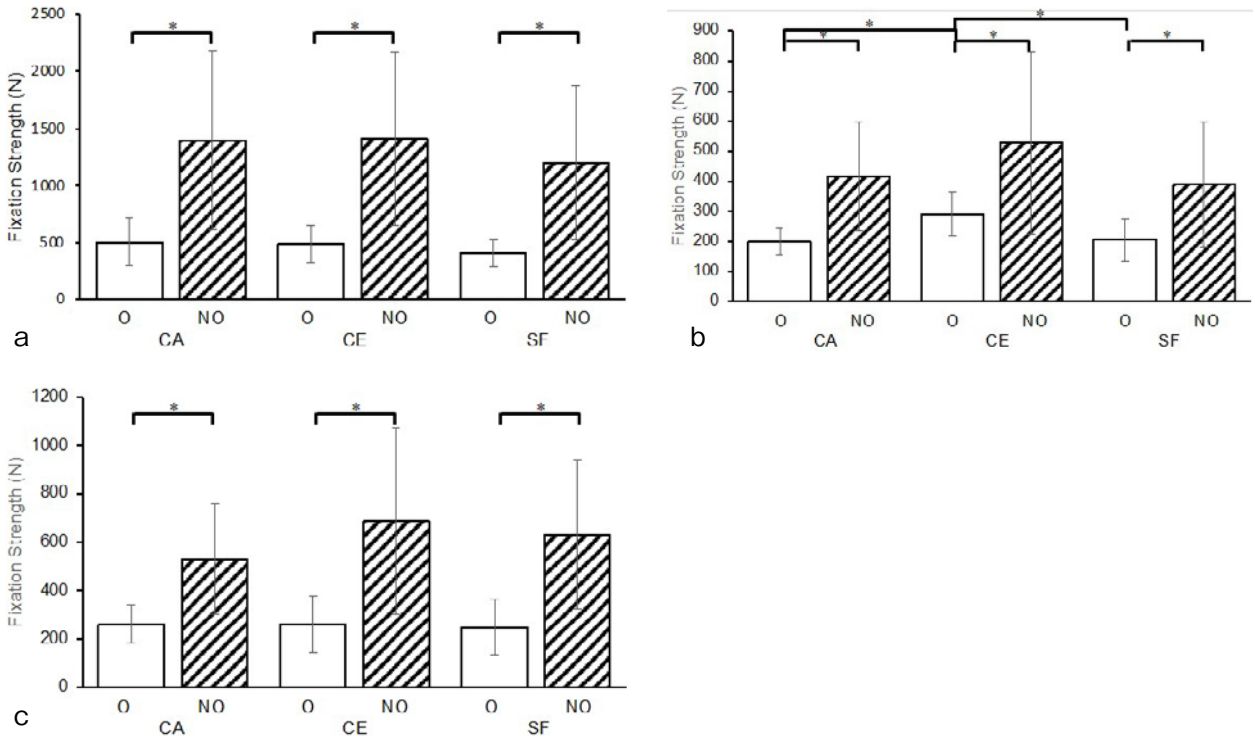

Figure 4. Comparison of the fixation strength of pedicle screws among caudal (CA), cephalad (CE), and straightforward (SF) trajectories in osteoporotic (O) and nonosteoporotic (NO) vertebrae against axial pullout (a), craniocaudal (b), and lateromedial (c) loads.

fold greater with statistically significant difference in all trajectories against each external load (axial pullout: P=0.004 for the CA, 0.003 for the CE, and 0.003 for the SF trajectories; craniocaudal: P=0.003 for the CA, 0.038 for the CE, and 0.022 for the SF trajectories; lateromedial: P=0.004 for the CA, 0.006 for the CE, and 0.003 for the SF trajectories) compared with the O group (Fig. 4). In the NO group, the FS of the PSs was not statistically significantly different between the trajectories for any of the external loads (Fig. 4). However, in the O group, the FS against the craniocaudal load in the CE trajectory was statistically significantly greater than those in the CA (P=0.016) and SF (P=0.023) trajectories, although this trend was not observed against the axial pullout and lateromedial loads (Fig. 4). The equivalent stress distribution around the bicortical PSs in each trajectory against external loads is presented in Fig. 5, with the

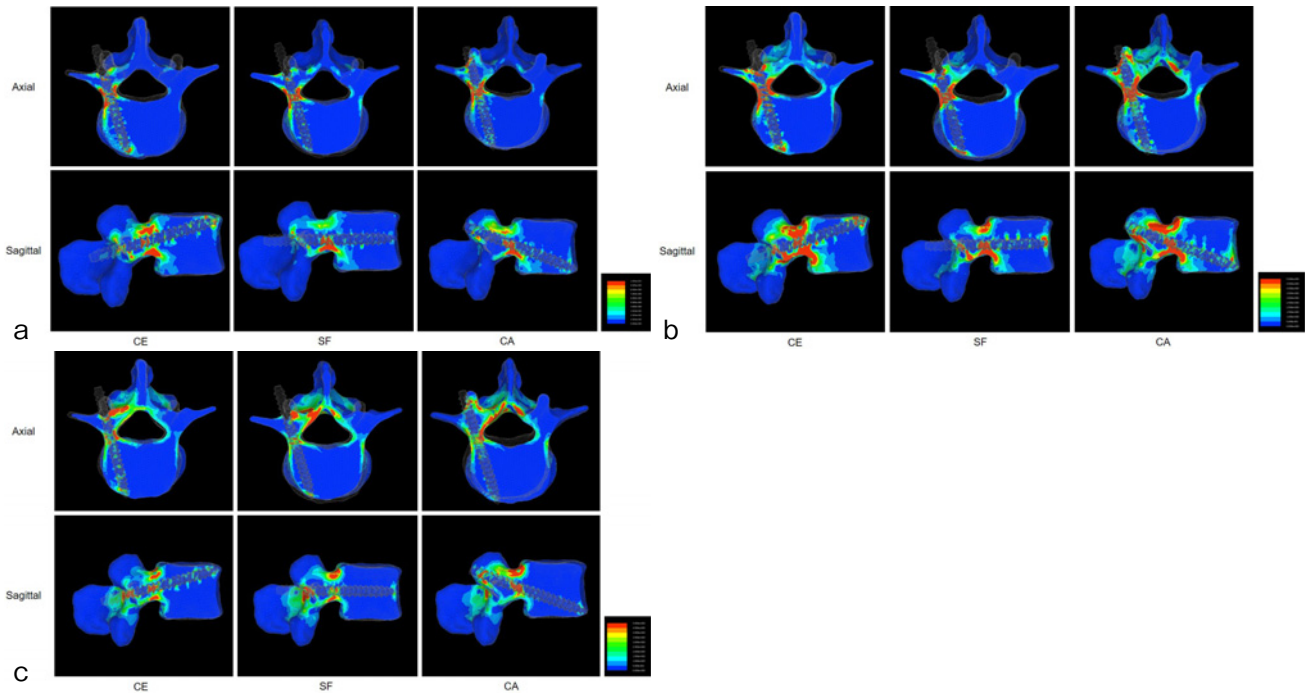

Figure 5. Distribution of Dragger–Prager equivalent stress on osteoporotic vertebrae in a representative case. Axial (upper row) and sagittal (bottom row) images against axial pullout (a), craniocaudal (b), and lateromedial (c) loads.

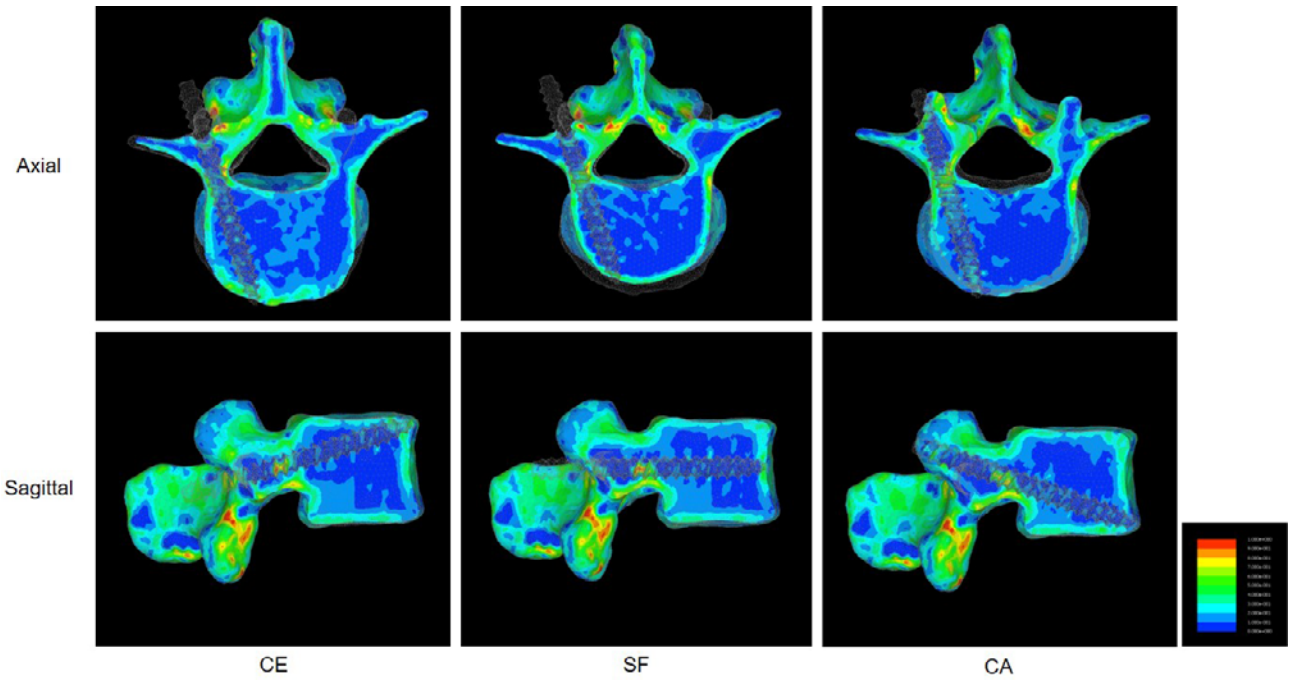

Figure 6. Illustrative case. Bone density (g/cm^3) distribution of the osteoporotic vertebra in the axial (upper row) and sagittal (lower row) planes.

red area indicating stress concentration. The pedicle mostly contributed to the FS of the PSs in all trajectories against all external loads, but in the CE trajectory, the anterior cortical bone layer at the screw tip exhibited a relatively higher stress distribution against all external loads than those in the CA and SF trajectories.

Discussion

This study applied three external loads on the PSs. The motions of the lumbar spine consist of flexion-extension, axial rotation, and side-bending. Craniocaudal and lateromedial loads may reflect flexion-extension and axial rotation, respectively. Regardless of the trajectory and type of external load, the bicortical PSs were superior to the unicortical PSs

in terms of the FS for both the osteoporotic and nonosteoporotic vertebrae. A recent biomechanical study that used osteoporotic lumbar vertebrae reported that the bicortical PSs had substantially greater pullout strength than the midbody PSs[23]. Another biomechanical study that used finite element models of osteoporotic lumbar vertebrae reported that longer PSs had greater FS against flexion, extension, lateral bending, and axial rotation forces applied to the vertebrae[24]. The results of the aforementioned studies corroborate our finding on the optimal depth of PSs.

Regarding our findings on trajectory, the FS was not considerably different for any of the trajectories against any of the external loads in the nonosteoporotic vertebrae. However, in the osteoporotic vertebrae, the PSs in the CE trajectory had substantially greater FS against the craniocaudal load than in the other trajectories, although no remarkable difference in the FS among the trajectories was observed against axial pullout and lateromedial loads. Previous *in vivo* studies that measured the load on PSs reported that the primary load was in a craniocaudal direction rather than in an axial pullout direction[25,26]. The axial pullout load was traditionally applied to assess the FS of PSs in biomechanical studies. However, a recent cadaveric study reported that nonaxial loads applied to PSs caused screw plowing, which led to subsequent screw loosening[27]. Finite element analyses also revealed that axial pullout did not substantially contribute to screw loosening and that craniocaudal loading increased the risk of screw loosening in the osteoporotic vertebrae[15,16]. The cortical bone layer exerts a substantial effect on the FS of PSs[28]. In addition, the strength of the vertebra-screw interface is associated with the regional bone density around PSs[29,30]. In the osteoporotic vertebrae in our cohort, the bone density at the screw tip of the PSs in the CE trajectory was greater than those in the CA and SF trajectories (Fig. 6). Therefore, bicortical PSs were recommended in the CE trajectory for the osteoporotic vertebra, although the trajectory did not affect the FS of PSs in the nonosteoporotic vertebra.

This study used finite element models developed from the preoperative CT images of the patients. Finite element analysis can negate the inherent disadvantages in biomechanical studies using animal or cadaveric bones. PSs with the same screw design, including thread shape, can be repeatedly inserted into a model in several trajectories, which leads to the reduction of bias in the quality of PSs and bones. The present study has several limitations that need to be acknowledged. First, the same equation was used for both osteoporotic and nonosteoporotic vertebrae. The equation includes bone density but not bone quality. Bone strength is defined as a combination of bone density and quality. For a more accurate analysis, models developed using micro-CT data are needed. Second, the external loading conditions do not accurately reflect clinical loading conditions. Surgically embedded implants including PSs are exposed to repetitive biomechanical stresses inside the body due to the patient's daily movements. Therefore, cyclic loading to PSs might be needed to assess FS in vertebral models, as mentioned in a previous study[16]. Third, the insertion techniques did not completely reflect those employed in clinical settings, in which the pedicle is probed and a tapping hole is created. Finally, models with instrumentation at multiple vertebrae were not used. In spine surgery, PSs are connected to rods at multiple vertebrae. To the best of our knowledge, this is the first study to investigate the optimal depth and trajectory of PSs in osteoporotic and nonosteoporotic vertebrae against various external loads.

In conclusion, our results indicate that bicortical PSs should be selected for spinal instrumentation in patients with and without osteoporosis. In patients with osteoporosis, PSs should be inserted in the trajectory toward the superior-anterior corner of the vertebra.

Conflicts of Interest: The authors declare that there are no relevant conflicts of interest.

Sources of Funding: None.

Acknowledgement: We also acknowledge the proofreading and editing by Benjamin Phillis at the Clinical Study Support Center at Wakayama Medical University.

Author Contributions: A.M. and S.T. designed the study; A.M. performed the experiments and analyzed the data; A.M. and S.T. wrote the manuscript; E.Y., T.K., R.N., and H.Y. supervised the experiments. All authors have read and approved the final manuscript.

Ethical Approval: This study was approved by the Wakayama Medical University Ethics Committee (Approval code: 3800).

Informed Consent: Informed consent for publication was obtained from all participants.

References

1. Boucher HH. A method of spinal fusion. J Bone Joint Surg Br. 1959;41-B(2):248-59.
2. Steffee AD, Biscup RS, Sitkowski DJ. Segmental spine plates with pedicle screw fixation. A new internal fixation device for disorders of the lumbar and thoracolumbar spine. Clin Orthop Relat Res. 1986;203(203):45-53.
3. Dickman CA, Fessler RG, MacMillan M, et al. Transpedicular screw-rod fixation of the lumbar spine: operative technique and outcome in 104 cases. J Neurosurg. 1992;77(6):860-70.
4. Kumano K, Hirabayashi S, Ogawa Y, et al. Pedicle screws and bone mineral density. Spine. 1994;19(10):1157-61.
5. Ohlin A, Karlsson M, Düppe H, et al. Complications after transpedicular stabilization of the spine. A survivorship analysis of 163 cases. Spine. 1994;19(24):2774-9.
6. Pihlajämaki H, Myllynen P, Böstman O. Complications of transpedicular lumbosacral fixation for non-traumatic disorders. J Bone Joint Surg Br. 1997;79(2):183-9.
7. Glaser J, Stanley M, Sayre H, et al. A 10-year follow-up evaluation of lumbar spine fusion with pedicle screw fixation. Spine.

2003;28(13):1390-5.
8. Wu ZX, Gong FT, Liu L, et al. A comparative study on screw loosening in osteoporotic lumbar spine fusion between expandable and conventional pedicle screws. Arch Orthop Trauma Surg. 2012; 132(4):471-6.
9. Cho W, Cho SK, Wu C. The biomechanics of pedicle screw-based instrumentation. J Bone Joint Surg Br. 2010;92(8):1061-5.
10. Zindrick MR, Wiltse LL, Widell EH, et al. A biomechanical study of intrapeduncular screw fixation in the lumbosacral spine. Clin Orthop Relat Res. 1986;203(203):99-112.
11. Weinstein JN, Rydevik BL, Rauschning W. Anatomic and technical considerations of pedicle screw fixation. Clin Orthop Relat Res. 1992;284(284):34-46.
12. Wu SS, Edwards WT, Yuan HA. Stiffness between different directions of transpedicular screws and vertebra. Clin Biomech (Bristol, Avon). 1998;13:S1-8.
13. Yuan Q, Han X, Han X, et al. Krag versus caudad trajectory technique for pedicle screw insertion in osteoporotic vertebrae: biomechanical comparison and analysis. Spine. 2014;39(26):B27-35.
14. Shibasaki Y, Tsutsui S, Yamamoto E, et al. A bicortical pedicle screw in the caudad trajectory is the best option for the fixation of an osteoporotic vertebra: an in-vitro experimental study using synthetic lumbar osteoporotic bone models. Clin Biomech (Bristol, Avon). 2020;72:150-4.
15. Fasser MR, Gerber G, Passaplan C, et al. Computational model predicts risk of spinal screw loosening in patients. Eur Spine J. 2022;31(10):2639-49.
16. Song F, Liu Y, Fu R, et al. Craniocaudal toggling increases the risk of screw loosening in osteoporotic vertebrae. Comput Methods Programs Biomed. 2023;238:107625.
17. Duan PG, Mummaneni PV, Rivera J, et al. The association between lower Hounsfield units of the upper instrumented vertebra and proximal junctional kyphosis in adult spinal deformity surgery with a minimum 2-year follow-up. Neurosurg Focus. 2020;49(2): E7.
18. Schreiber JJ, Anderson PA, Rosas HG, et al. Hounsfield units for assessing bone mineral density and strength: a tool for osteoporosis management. J Bone Joint Surg Am. 2011;93(11):1057-63.
19. Zou D, Li W, Deng C, et al. The use of CT Hounsfield unit values to identify the undiagnosed spinal osteoporosis in patients with lumbar degenerative diseases. Eur Spine J. 2019;28(8):1758-66.
20. Imai K, Ohnishi I, Yamamoto S, et al. In vivo assessment of lumbar vertebral strength in elderly women using computed tomography-based nonlinear finite element model. Spine. 2008;33 (1):27-32.
21. Keyak JH, Rossi SA, Jones KA, et al. Prediction of femoral fracture load using automated finite element modeling. J Biomech. 1998;31(2):125-33.
22. Chao CK, Hsu CC, Wang JL, et al. Increasing bending strength and pullout strength in conical pedicle screws: biomechanical tests and finite element analyses. J Spinal Disord Tech. 2008;21(2):130-8.
23. Karami KJ, Buckenmeyer LE, Kiapour AM, et al. Biomechanical evaluation of the pedicle screw insertion depth effect on screw stability under cyclic loading and subsequent pullout. J Spinal Disord Tech. 2015;28(3):E133-9.
24. Matsukawa K, Yato Y, Imabayashi H. Impact of screw diameter and length on pedicle screw fixation strength in osteoporotic vertebrae: A finite element analysis. Asian Spine J. 2021;15(5):566-74.
25. Graichen F, Bergmann G, Rohlmann A. Patient monitoring system for load measurement with spinal fixation devices. Med Eng Phys. 1996;18(2):167-74.
26. Rohlmann A, Bergmann G, Graichen F. Loads on an internal spinal fixation device during walking. J Biomech. 1997;30(1):41-7.
27. Bianco RJ, Aubin CE, Mac-Thiong JM, et al. Pedicle screw fixation under nonaxial loads: A cadaveric study. Spine. 2016;41(3): E124-30.
28. Santoni BG, Hynes RA, McGilvray KC, et al. Cortical bone trajectory for lumbar pedicle screws. Spine J. 2009;9(5):366-73.
29. Myers BS, Belmont PJ Jr, Richardson WJ, et al. The role of imaging and in situ biomechanical testing in assessing pedicle screw pull-out strength. Spine. 1996;21(17):1962-8.
30. Hirano T, Hasegawa K, Takahashi HE, et al. Structural characteristics of the pedicle and its role in screw stability. Spine. 1997;22 (21):2504-9; discussion 2510.